Mikrochim. Acta 114/115, 175–185 (1994)

Mikrochimica Acta

© Springer-Verlag 1994
Printed in Austria

Electron and Ion Beam Analysis of Composition and Strain in $Si_{1-x}Ge_x$/Si Heterostructures

Aldo Armigliato[1,*], Donato Govoni[1], Roberto Balboni[2], Stefano Frabboni[2], Marina Berti[3], Filippo Romanato[4], and Antonio V. Drigo[4]

[1] CNR-Istituto LAMEL, Via P. Gobetti 101, I-40129 Bologna, Italy
[2] Dipartimento di Fisica dell'Universita', Via Campi 213/A, I-41100 Modena, Italy
[3] Dipartimento di Elettronica per l'Automazione, Facolta' di Ingegneria dell'Universita', Via Branze 38, I-25123 Brescia, Italy
[4] Dipartimento di Fisica dell'Universita', Via Marzolo 8, I-35131 Padova, Italy.

Abstract. $Si_{1-x}Ge_x$ heterostructures have been grown by molecular beam epitaxy, with nominal compositions of 10 and 15 at %. Analytical electron microscopy, Rutherford backscattering spectrometry and ion channeling have been used in order to determine film thickness, Ge molar fraction and tetragonal distortion. The actual Ge concentrations were found to be smaller than the nominal ones. For all the SiGe films a coherent growth was found, with a small deviation from the perfect tetragonal distortion. The good agreement found between the results obtained by each analytical technique demonstrate that these methods of characterization are powerful tools for the control of the epitaxial layer parameters.

Key words: silicon-germanium alloys, composition determination, lattice strain determination, convergent beam electron diffraction, ion beam analysis.

1. Introduction

Silicon-germanium alloys are presently receiving considerable attention due to the progress in the growth of strained coherent SiGe layers on silicon, which has made bandgap engineering possible in silicon technology. The feasibility of SiGe-based heterojunction bipolar transistors (HBTs) has been demonstrated a few years ago [1]. Other device structures such as FETs and optoelectronic detectors have also been demonstrated. Recently HBTs have been produced with high transit frequencies up to 75 GHz [2] and low base sheet resistivities down to 0.3 kohm/□ for a 50 nm thick base [3]. The thickness of the $Si_{1-x}Ge_x$ layer is an important device design parameter. The maximum thickness for pseudomorphic growth (critical thickness) of the alloy is strongly related to the Ge atomic fraction x. Moreover,

* To whom correspondence should be addressed

the bandgap width of the alloy depends on the value of the lattice strain, which, in turn, considerably affects the transit time of the electrons in the base region. Therefore thickness, Ge concentration and lattice strain of the SiGe thin films are parameters that must be accurately determined and controlled.

$Si_{1-x}Ge_x$ films grown on Si by molecular beam epitaxy (MBE) have been analysed by analytical electron microscopy (AEM) and by Rutherford backscattering spectrometry (RBS) and ion channeling. In AEM the Ge concentrations have been determined by energy dispersive X-ray spectrometry (EDS) and the lattice strain by convergent beam electron diffraction (CBED) and large angle convergent beam electron diffraction (LACBED). The RBS measurement of the chemical profile in the samples is complemented by the analysis of their plastic and elastic deformation performed in channeling condition.

2. Sample Preparation

$Si_{1-x}Ge_x$ alloys were grown by conventional solid source MBE. The details of the growth have been described before [4]. Briefly, Si and Ge are each evaporated from electron beam sources that are individually closed loop controlled. The substrate temperature is independently controlled by radiant heating from behind the wafer. As described elsewhere [5] the growth of abrupt Si/SiGe structures requires low temperatures. The films employed in this study were typically grown at 550°C at growth rates of about 0.5 nm/s. Prior to growth the Si(100) wafers were RCA cleaned and in situ cleaned at temperatures of about 900°C for 20 min. This resulted in an atomically clean surface on which a thin (typically 100 nm) Si buffer was grown at 650°C. The temperature was then ramped down and the SiGe layer was grown. The nominal features of the specimens investigated are: $x = 15\%$ and $t = 100$ nm for specimen SIGE5, $x = 10\%$ and $t = 500$ nm for specimen SIGE6 and $x = 10\%$ and $t = 100$ nm for specimen SIGE7.

3. Analytical Electron Microscopy

3.1. Experimental

TEM [001] plan-sections and [100] cross-section of the various heterostructures were analysed. TEM cross-sections were prepared according to a procedure [6] that involves glueing, sawing, mechanical lapping down to 20 μm, and ion-beam milling to perforation. For the X-ray microanalysis the cross-sections were preferred to the corresponding plan-sections. In fact, in this case the contribution to the analysed volume from the silicon substrate, which would affect the determination in a rather unpredictable way, can easily be avoided. TEM plan-sections were first mechanically thinned down to 20 μm and then ion milled to perforation.

The TEM specimens were investigated by using a Philips CM 30 TEM, equipped with an EDAX PV9900 (EDS). The accelerating voltage was 300 kV for imaging, X-ray analysis and LACBED purposes, and 100 kV for the CBED experiments. A Gatan liquid-nitrogen cooled double tilt holder was employed. The spot size at the specimen level was 10 nm, obtained in the nanoprobe mode; this mode of operation is particularly advantageous in EDS analyses, because it minimises the contribution to the X-ray signal coming from the electrons backscattered from the lower pole pieces of the objective lens. The analysed volume was of the order of 10^{-4} μm^3.

3.2. Morphology and Structure

Two XTEM micrographs showing the morphology of samples SIGE6 and SIGE7 are presented in Figs. 1a and 1b. Sample SIGE6 has grown without threading

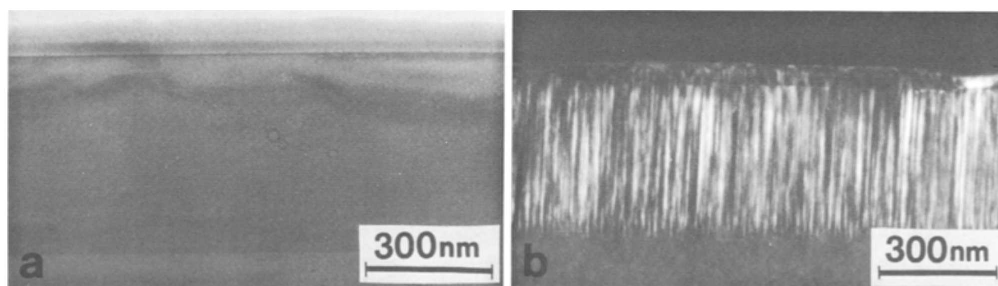

Fig. 1. **a** XTEM bright field image of sample SIGE6, and **b** XTEM dark field image ($g = (004)$) of sample SIGE5

dislocations and with a sharp interface with the buffer. No misfit dislocations are detected in plan-thinned samples, so a coherent growth can be assumed.

Somewhat different is the situation in samples SIGE7 and SIGE5, as shown in Fig. 1b which refers to the latter. In these heterostructures contrast features extending from the SiGe/buffer interface to the surface are clearly detected. This contrast, on the basis of diffraction contrast experiments (visibility with $g = (004)$ parallel to the growth direction, extinction with $g = (040)$ normal to the growth direction), can be reasonably ascribed to small strain variations between adjacent columns of SiGe film, and not to structure factor contrast. No dislocations (threading and/or misfit) are detected in both plan and cross-sectioned specimen, so a coherent growth can also be assumed for these samples.

3.3. X-Ray Microanalysis

The film composition has been determined by TEM/EDS at 300 kV in the nanoprobe mode. The choice of the maximum accelerating voltage available in our microscope is dictated by the increase in the peak-to-background ratio and the corresponding decrease, with increasing beam energy, of beam broadening, thus improving the analytical accuracy and spatial resolution. To obtain the Ge concentration in the various SiGe films, a previously reported analytical method was employed [7–8]. Basically, it consists of the intensity measurement of the SiKα and GeKα X-ray peaks generated in the SiGe film at two different tilt angles (0° and 20°). This method, which allows one to obtain simultaneously the composition and thickness of a thin film, requires the experimental determination of the intensity ratio, $R_m = I(\text{SiK}_\alpha)/I(\text{GeK}_\alpha)$ at the two tilt angles and makes use of two computer programs. The first code, named CARLONE, is a Monte Carlo simulation based on the single scattering approach and the continuous slowing down approximation. It generates two sets of computed ratios $R_c = I(\text{SiK}_\alpha)/I(\text{GeK}_\alpha)$ for the two tilt angles, as a function of the Ge concentration, x, and mass thickness ρt [mg/cm^2]. A procedure similar to the one proposed by Kyser and Murata [9] enables one to determine the x and ρt values which minimize the difference $|R_c(x, \rho t) - R_m|$ for the two tilt angles. Such a method, codified in the second program, ROSIN, does not need standard samples for reference, provided the X-ray absorption in the beryllium window of the detector is known. In Fig. 2 the result of the minimization procedure in the case of sample SIGE5 is reported. The experimental intensity ratios R_m were

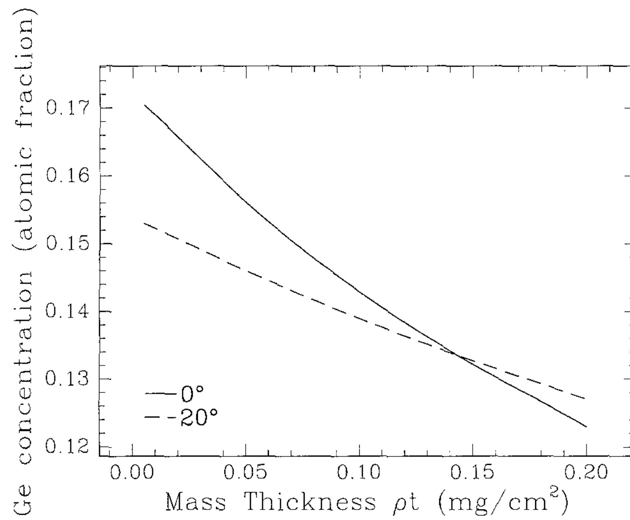

Fig. 2. Germanium concentration as a function of the local mass thickness, ρt, for the SIGE5 film. The two curves correspond to the X-ray spectra taken at tilt angles of 0° and 20°

3.23 ± 0.07 and 3.70 ± 0.07 for 0° and 20° of tilt, respectively. The crossover of the curves, corresponding to the two tilt angles, gives the Ge concentration and the local thickness of the cross section. Although this latter parameter is of no practical importance (the relevant thickness being that of the original SiGe film, which is immediately deduced from the width of the corresponding stripe in the cross-sectional image), the existence of a crossover in plots like the ones in Fig. 2 is not a priori predictable and is therefore a test of the quality of the experimental measurements. By considering the errors in beam repositioning when tilting from one angle to the other and back, as well as the statistical uncertainties, an overall experimental error smaller than 2% can be estimated. The X-ray analysis of sample SIGE6 revealed that the Ge concentration was not constant along the film depth; namely, that there were two distinct regions of different composition, the border being located at about 100 nm from the SiGe/substrate interface, as seen in Fig. 1a. The data on the Ge concentration in the investigated SiGe films are summarized in Table 1.

Table 1. Germanium concentration C, film thickness t and tetragonal distortion ε^T in the different $Si_{1-x}Ge_x$ films, as deduced from analytical electron microscopy (AEM) and Rutherford backscattering spectrometry (RBS)

	C(Ge) (at.%)		t(nm)	ε^T (AEM) (%)			$f(1+\alpha)-\varepsilon^T$ (%)	
Sample	EDS	RBS		CBED	LACBED	ε^T (RBS)	LACBED	RBS
SIGE5	13.4±0.4	13.4±0.3	447±5	0.83±0.09	0.85±0.04	0.85±0.03	0.06±0.05	0.06±0.04
SIGE6	7.7±0.4	7.7±0.3	385±5	0.50±0.05	0.50±0.04	0.45±0.03	0.04±0.05	0.08±0.04
	6.3±0.4	6.1±0.3	100±5					
SIGE7	7.7±0.4	7.7±0.3	109±5	0.46±0.05	0.42±0.04	0.45±0.03	0.10±0.05	0.08±0.04

EDS = energy dispersive spectrometry; CBED = convergent beam electron diffraction; LACBED = large angle CBED. The quantity $f(1+\alpha)$ is the value of tetragonal distortion for a perfect pseudomorphic growth, hence $f(1+\alpha)-\varepsilon^T$ gives the strain release of the films. Note that SIGE6 exhibits two regions of different composition.

3.4. Convergent Beam Electron Diffraction Analysis CBED and LACBED

The tetragonal strain is defined as $\varepsilon^T = \frac{a^{\perp}_{SiGe}}{a^{=}_{SiGe}} - 1$, where $a^{\perp}_{SiGe}$ and $a^{=}_{SiGe}$ are the lattice constants along directions perpendicular and parallel, respectively, to the wafer surface (for coherent structures $a^{=}_{SiGe} = a_{Si}$). The values of ε^T of the various heterostructures have been measured by convergent beam electron diffraction techniques named CBED [10] and LACBED [11].

In the first case the tetragonal strain has been measured through the variation of high order Laue zone (HOLZ) lines position in the central disc of a [130] convergent beam diffraction pattern taken at 100 kV. In order to quantify the unknown lattice parameter variations between the strained SiGe film and the silicon substrate, the silicon experimental pattern is first matched with a kinematically simulated one (EMS routine by Stadelmann [12]) taking the acceleration voltage as a fitting parameter while the silicon lattice constant is assumed to be 0.5429 nm which is the value at the temperature of observation (100 K). Then the unknown lattice parameters of the SiGe films are determined by fitting the experimental pattern with the calculated one, taking the SiGe lattice constants as fitting parameters. The experimental and calculated HOLZ-line patterns relative to the SIGE5 and SIGE7 samples are reported in Fig. 3. It is interesting to correlate the CBED patterns with the morphology observed in diffraction contrast experiments; in particular by considering the sharpness of the lines, which is a test for the crystal

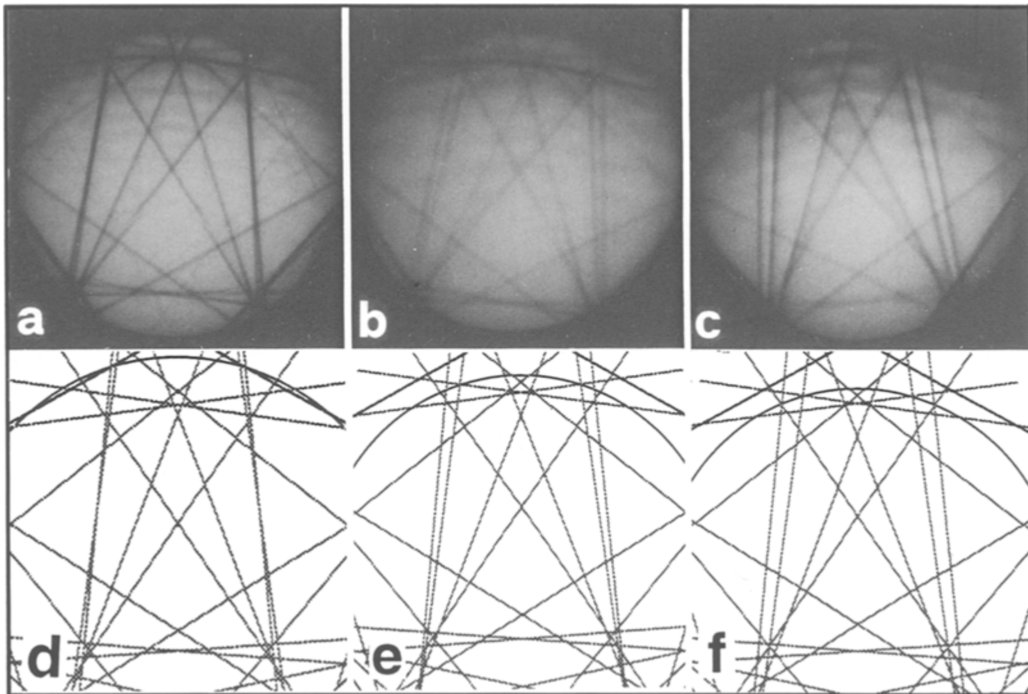

Fig. 3. a–c [130] experimental HOLZ-line patterns relative to the silicon substrate, to SIGE5, and to the SIGE7 film. **d–f** Corresponding kinematically computed patterns. Acccleration voltage: 100 kV. Analyses performed at 100 K

quality, it is reasonable to assume that the contrast features observed in Fig. 1b are produced by a strain lower than the sensitivity of the CBED technique ($2 \cdot 10^{-4}$).

The HOLZ-line method is particularly suitable in cross-sectioned samples, since the interface between the substrate and the SiGe film is parallel to the viewing direction, and so distinct HOLZ-line patterns from the substrate and the strained layers can be independently recorded in sequence. With this method it is possible to determine with high accuracy the quantity $\varepsilon^{\perp}_{CBED} = \frac{a^{\perp}_{SiGe_{CBED}}}{a_{Si}} - 1$ measured on the thinned specimen where a relaxation of the stress along the thinning direction and the consequent modification of the strain field could occur. As we have found in previous experiments [13] the amount of this modification depends on the local thickness of the specimen and on the distance of the analysed region from the SiGe/buffer interface. However for thicknesses suitable for CBED measurements (about 300 nm) and for distances from the interface greater than 50 nm we have found that the ratio between $\varepsilon^{\perp}_{CBED}$ and ε^{T} is 0.80 ± 0.08, a value slightly higher than that relative to the fully relaxed case ($2/(2 + \alpha) = 0.72$, where $\alpha = 2 \cdot C_{12}/C_{11}$, with C_{12}, C_{11} two of the stiffness constants of the material [14]). By means of this correction factor we can estimate ε^{T} with an accuracy of about 10%. These values are reported in Table 1 for all the three samples investigated.

The difficulties associated with strain quantification in cross-sectioned samples can be overcome by using the LACBED technique in plan-sections, where relaxation phenomena are smaller [11]. This technique directly measures the rotation of the planes inclined at a particular angle θ with respect to the surface which is caused by the tetragonal distortion of the cubic lattice. The amount of rotation is related to the ε^{T} with the relation:

$$2\Delta\theta = \varepsilon^{T} \sin(2\theta). \quad (1)$$

The tetragonal strain can therefore be readily obtained by measuring $\Delta\theta$. This can be achieved by means of the LACBED technique because both the unperturbed and the tilted planes may be observed in their Bragg position owing to the large illumination angle used. Thus a rocking curve is obtained for each plane, and Bragg contour deficiency lines are observed in the transmitted beam; if a strained layer is present, medium and high index reflections show a split central peak. $\Delta\theta$ can therefore be measured from a single diffraction pattern. Figures 4a and b show direct beam LACBED [012] zone axis patterns from the SIGE5 and SIGE7 specimens. It is clearly seen that the (084) and (242) Bragg contours relative to planes inclined with respect to the [001] sulface are split, whereas the (800) Bragg contour relative to the plane parallel to the surface is unsplit. From these LACBED patterns we have deduced ε^{T} according to Eq. (1). The measured values are reported in Table 1.

It is useful to consider the value that the tetragonal distortion should have for a perfect pseudomorphic growth, $f(1 + \alpha)$ where f is the misfit, defined as

$$f = \frac{a_{SiGe}}{a_{Si}} - 1. \quad (2)$$

We calculated f taking into account the deviation of a_{SiGe} from the Vegard law [15], for all the three samples. The difference between $f(1 + \alpha)$ and ε^{T}, reported in Table

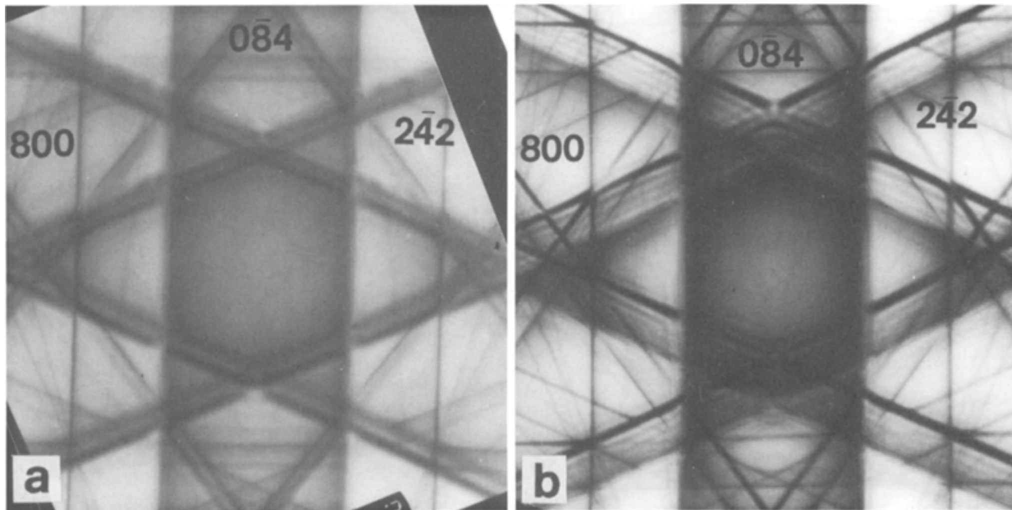

Fig. 4. a, b [012] zone axis LACBED pattern taken on the sample SIGE7 and SIGE5 at 300 kV. Splitting of the (084) and (242) Bragg contours is evident. The (800) Bragg contour is unsplit

1, measures the efficiency of the lattice defects to release the elastic energy accumulated in the elastic distortion of the lattice.

4. Rutherford Backscattering Spectrometry and Ion Channeling

4.1. Experimental

The Rutherford backscattering spectrometry (RBS) spectra were recorded to check the thickness and the composition of the layers. They were collected using a 2.0 MeV $4He^+$ beam produced by the 2.3 MV Van der Graaff accelerator placed at the Laboratori Nazionali di Legnaro. The charge collection measurement was performed using the scattering chamber as a Faraday cup and was accurate to better than 1%. In the case of the thinner film sample (SIGE7, nominally 100 nm thick) the scattering angle was chosen equal to 120° in order to have a good thickness resolution. The RBS measurements were calibrated in solid angle against Ta/Si standard samples, whose absolute Ta content was known with an accuracy better than 2% [16]. A high precision goniometric sample holder was used to perform the channeling analysis. Three rotation axes allow complete freedom of orientation of the sample with respect to the beam. Two linear translations make it possible to change the beam spot position on the sample surface in order to avoid radiation damage accumulation while keeping the analysed point at the intersection of the three rotation axes. All the movements are made by independent and fully computer controlled stepping motors. One step corresponds to 0.01° for each of the rotation axes and the repeatability and the overall precision are both 0.01°.

4.2. Composition Determination

The depth concentration profile of the $Si_{1-x}Ge_x$ alloys was determined by using a computer program able to simulate the RBS spectra of the samples. As this program

does not take into account any channeling effect, the sample was rotated during the collection of the spectra in such a way that the beam direction described a cone around the growth axis [001]. It has been shown that this, averaged over each angular position, results in a good approximation to a random spectrum in a crystal lattice [13].

The RBS simulation program takes a trial concentration profile as input and the actual profile is reached when the simulated spectrum is within the statistical fluctuation of the experimental spectrum. In the case of our samples, the constraint of the complementary atomic fractions of Ge, x, and of Si, makes x the only fitting parameter used to determine the composition. In fact, any change in x produces height changes in the Ge and in the Si signals in opposite directions allowing the composition to be determined. Clearly high precision is reached if the statistics of the signal is good enough. However, it makes no sense to increase the statistics of the signal in order to have the precision of the determination better than the accuracy. The latter has a small dependence on systematic errors associated with the stopping power function of the $^{+}He^{4}$ particles in the material. The best choice [17, 18] of the stopping power function was dealt with in a previous work [13], where also the errors in the thickness determination were discussed. For this kind of samples the value of x can be determined with an error of about 0.3 at %, while the thickness uncertainty of films with sharp interfaces is of the order of 5 nm. The random spectra of the three considered samples and the simulated spectrum of one of them (SIGE6) are shown in Fig. 5. The simulated spectrum for SIGE6 is shown because in this sample the Ge concentration varied with film thickness as already

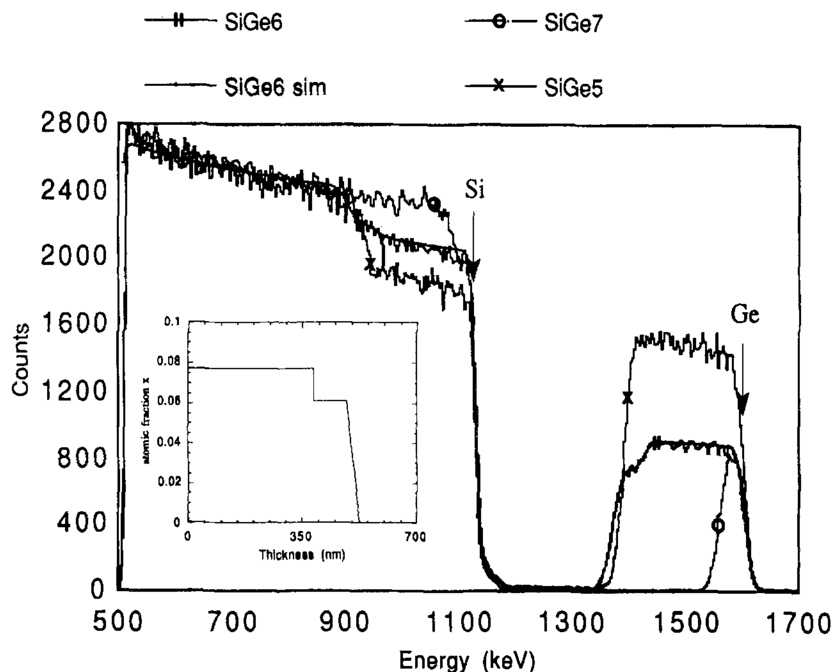

Fig. 5. Comparison of the random spectra of the three analysed samples. The inset shows the chemical profile used to calculate the simulated SIGE6 spectrum which is also included for comparison. The arrows mark the backscattering energy from Ge and Si at the surface

noted in section 3.3. The good agreement between the simulation and the experimental spectrum was obtained taking into account the energy resolution of the detector and the presence of the Ge and Si isotopes with their relative abundances.

Contrary to the case of SIGE6, the spectra of samples SIGE5 and SIGE7 were simulated with step functions of the chemical profile. In these two specimens the width of the Ge signal edges is due to the experimental resolution, indicating that the SiGe interface is sharper than the RBS depth resolution.

4.3. Channeling Analysis

The analysis of the crystalline quality of the samples was performed by recording the RBS spectra along the [001] direction and along the (110) planar direction at 5° from the [001] axis. Afterwards the dechanneling fraction χ was calculated, i.e. the yield of the channeling spectrum with respect to the random spectrum. In Fig. 6 the planar and axial χ function spectra of the sample SIGE5 are compared to the corresponding χ function of a Si virgin sample. The oscillations of the planar χ function of the film signal mimic those of the virgin Si, indicating that the lattice quality of the sample was rather good. Nevertheless, the lattice was not perfect, as demonstrated by the progressively higher dechanneling both in the axial and in the planar configurations. A similar behaviour was found for SIGE7, while SIGE6 exhibited an almost perfect lattice structure. In this latter sample only a small difference from the reference curve was observed near the interface region.

The analysis of the structure of the film by channeling was complemented by the determination of the lattice distortion. The method used for this analysis was based on a high-precision measurement of the absolute angular position of many axial and planar channeling minima [19]. The value of the ratio between the lattice

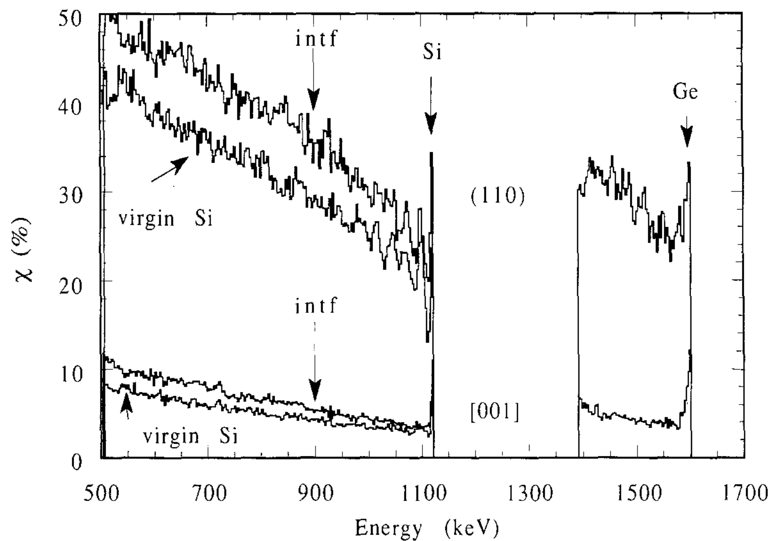

Fig. 6. Dechanneling function of the planar (110) and of the axial [001] channeling spectra of the sample SIGE5. The specimen surface (*Si* and *Ge*) and the SiGe/Si interface (*intf*) are indicated. As a reference, the dechanneling function of virgin Si is included

parameter perpendicular and parallel to the interface, $\frac{a_{\mathrm{SiGe}}^{\perp}}{a_{\mathrm{SiGe}}^{=}}$, was obtained from a least squares fit of all the measured channeling minima. This procedure allowed the tetragonal distortion of the unit cell to be determined. The values of the tetragonal distortion of all the samples are reported in Table 1, together with the values of $f(1+\alpha) - \varepsilon^{T}$.

5. Conclusions

The analytical techniques employed in this work (EDS, CBED, LACBED and RBS and ion channeling) have yielded values of the Ge concentration and lattice strain in the SiGe films in good mutual agreement.

In addition, TEM observations showed that the films SIGE5 and SIGE7 had a different morphology, from SIGE6, due to the presence of columnar, coherent grains with slightly different strain. This difference was clearly seen in the channeling spectra.

The measured Ge concentrations ranged from about 6 to 13 atomic % whereas the tetragonal strains varied from about 0.4 to 0.8 $\times$ 10^{-2}. From the comparison of Ge concentration and strain in the SiGe films, it has been possible to deduce the possible deviation from the perfect tetragonal distortion, i.e the strain release. This was small, yet detectable, both in the films SIGE5 and SIGE7 where columnar grains had formed and in SIGE6 which exhibited two regions of different composition. Thus both these features seem to be effective in inducing the small deviation from the perfect tetragonality, although the mechanism is not yet fully understood.

Acknowledgements. The authors are indebted to R. Rosa for the use of the Monte Carlo code for EDS microanalysis and to F. Corticelli for his skilful technical assistance. This work was partially supported by CNR, Progetto Strategico "Elettronica a Stato Solido".

References

[1] G. L. Patton, S. S. Iyer, S. L. Delage, S. Tiwari, J. M. C. Stork, *IEEE-ED Lett.* **1988**, *9*, 165.
[2] G. L. Patton, J. H. Comfort, B. S. Meyerson, E. F. Crabbe, G. J. Scilla, E. de Fresart, J. M. C. Stork, J. Y. C. Sun, D. L. Harame, J. N. Burghartz, *IEEE-ED Lett.* **1990**, *11*, 171.
[3] E. Kasper, H. Kibbel, U. Koenig, *Mat. Res. Soc. Symp. Proc.* **1991**, *220.*
[4] S. S. Iyer, in: *Epitaxial Silicon Technology* (B. J. Baliga, ed.), Academic Press, Orlando, FL, 1986.
[5] S. S. Iyer, J. C. Tsang, M. W. Copel, P. R. Pukite, R. M. Tromp, *Appl. Phys. Lett.* **1988**, *54*, 219.
[6] A. Garulli, A. Armigliato, M. Vanzi, *J. Microsc. Spectrosc. Electron.* **1985**, *10*, 135.
[7] R. Rosa, A. Armigliato, *X-Ray Spectrom.* **1989**, *18*, 19.
[8] A. Armigliato, R. Rosa, *Ultramicroscopy* **1990**, *32*, 127.
[9] D. F. Kyser, K. Murata, *IBM J. Res. Dev.* **1974**, *18*, 352.
[10] P. M. Jones, G. M. Rackham, J. W. Steeds, *Proc. R. Soc. Lond.* **1977**, *A 354*, 197.
[11] D. Cherns, A. R. Preston, *J. Electron Microsc. Tech.* **1989**, *13*, 111.
[12] P. Stadelmann, *Ultramicroscopy* **1987**, *21*, 131.
[13] A. Armigliato, M. Servidori, F. Cembali, R. Fabbri, R. Rosa, F. Corticelli, D. Govoni, A. V. Drigo, M. Mazzer, F. Romanato, S. Frabboni, R. Balboni, S. S. Iyer, A. Guerrieri, *Microsc. Microanal. Microstruct.* **1992**, *3*, 363.

[14] L. D. Landau, E. M. Lifshitz, *Theory of Elasticity*, Pergamon, New York, 1959.
[15] J. P. Dismukes, L. Ekstrom, R. J. Paff, *J. Phys. Chem.* **1964**, *68*, 3021.
[16] C. Cohen, J. AS. Davis, A. V. Drigo, T. E. Jackman, *Nucl. Instrum. Meth.* **1983**, *218*, 147.
[17] J. F. Ziegler, *Stopping Power and Ranges of Ions in Matter, Vol. 4*, Pergamon Press, New York, 1977.
[18] D. C. Santry, R. D. Werner, *Nucl. Instrum. Meth.* **1978**, *178*, 523.
[19] A. Carnera, A. V. Drigo, *Nucl. Instrum. Meth.* **1990**, *B44*, 357.